To appear in Proceedings of the 2nd Gauss Symposium, Springer-Verlag, 1994.

Local Regularization and Adaptive Methods for the Inverse Laplace Problem

Christopher R. Johnson[1] and Robert S. MacLeod[2]

[1]Department of Computer Science and [2]Cardiovascular Research and Training Institute
University of Utah, Salt Lake City, UT 84112
Email: crj@cs.utah.edu and macleod@vissgi.cvrti.utah.edu

Abstract

One of the fundamental problems in theoretical electrocardiography can be characterized by an inverse problem. We present new methods for achieving better estimates of heart surface potential distributions in terms of torso potentials through an inverse procedure. First, we outline an automatic adaptive refinement algorithm that minimizes the spatial discretization error in the transfer matrix, increasing the accuracy of the inverse solution. Second, we introduce a new local regularization procedure, which works by partitioning the global transfer matrix into sub-matrices, allowing for varying amounts of smoothing. This allows regularization parameters for each sub-matrix to be specifically 'tuned' using an *a priori* scheme based on the L-curve method. This *local* regularization method provides a substantial increase in accuracy when compared to global regularization schemes. We conclude with specific examples of these techniques using thorax models derived from MRI data.

Introduction

The intrinsic electrical activity of the heart gives rise to electric, and thus potential, fields within the volume of the thorax and upon the torso surface. The voltages on the torso surface are related to voltages upon the heart's surface via the resistive properties of the intermediary tissues (volume conductor). The general inverse problem in electrocardiography can be stated as follows: given a subset of electrostatic potentials measured on the surface of the torso and the geometry and conductivity properties of the thorax, calculate the potential fields on, and source currents, within, the heart. Mathematically this can be posed as an inverse source problem in terms of the primary current sources within the heart and described mathematically by Poisson's equation for electrical conduction:

$$\nabla \cdot \sigma \nabla \Phi = -I_v \quad \text{in } \Omega \tag{1}$$

with the boundary condition:

$$\sigma \nabla \Phi \cdot \mathbf{n} = 0 \quad \text{on } \Gamma_T \tag{2}$$

where Φ are the electrostatic potentials, σ is the conductivity tensor, I_v are the cardiac current sources per unit volume, and Γ_T and Ω represent the surface and the volume of the thorax, respectively. The goal is to recover the magnitude and location of the cardiac sources. In general, (1) does not have a unique solution. In order to solve the general source problem, one usually breaks up the volume of the heart into subregions within which simplifying assumptions are made regarding the form of the source term (such as dipoles or other equivalent sources). One then tries to recover information regarding the magnitude and direction of the simplified model sources.

Alternatively, one can solve for the electrostatic potentials on a surface bounding the heart. This form of the inverse problem does have a unique solution. Thus, instead of solving Poisson's equation, we solve a generalized Laplace's equation with Cauchy boundary conditions:

$$\nabla \cdot \sigma \nabla \Phi = 0 \tag{3}$$

with boundary conditions:

$$\Phi = \Phi_0 \quad \text{on } \Sigma \subseteq \Gamma_T \quad \text{and} \quad \sigma \nabla \Phi \cdot \mathbf{n} = 0 \quad \text{on } \Gamma_T. \tag{4}$$

While this version of the inverse problem has a unique solution [1], the problem is still mathematically ill-posed in the Hadamard sense; i.e., because the solution does not depend continuously on the data, small errors in the measurement of the voltages on the torso can yield unbounded errors in the solution.

An accurate solution to the inverse problem in electrocardiography would provide a noninvasive procedure for the evaluation for myocardial ischemia [2], the localization of ventricular arrhythmias and the site of accessory pathways in Wolff-Parkinson-White (WPW) syndrome, and, more generally, the determination of patterns of excitation and recovery of excitability.

Mathematical Theory

Finite Element Approximation

In order to solve the boundary value problem in (1) or (3) in terms of the epicardial potentials, we need to pose the problem in a computationally tractable way. This involves approximating the boundary value problem on a finite dimensional subspace and reformulating it in terms of a linear matrix equation. For this study we utilized the finite element method (FEM) to approximate the field equation and construct the set of matrix equations. Briefly, one starts with the Galerkin formulation of (1). Note that this includes the Dirichlet and Neumann boundary conditions,

$$(\sigma \nabla \Phi, \nabla \overline{\Phi}) = -(I_v, \overline{\Phi}), \tag{5}$$

where $\overline{\Phi}$ is an arbitrary test function, which can be thought of physically as a virtual potential field, and the notation $(\phi_1, \phi_2) \equiv \int_\Omega \phi_1 \phi_2 \, d\Omega$ denotes the inner product in $L_2(\Omega)$. We now use the finite element method to turn the continuous problem into a discrete formulation. First we discretize the solution domain, $\Omega = \bigcup_{e=1}^{N} \Omega_e$, and define a finite dimensional subspace, $V_h \subset V = \{\overline{\Phi} : \overline{\Phi} \text{ is continuous on } \Omega, \nabla \overline{\Phi} \text{ is piecewise continuous on } \Omega\}$. We define parameters of the function $\overline{\Phi} \in V_h$ at node points, $\alpha_i = \overline{\Phi}(x_i), i = 1, 2, \ldots, N$ and define the basis functions $\Psi_i \in V_h$ as linear piecewise continuous functions that take the value 1 at node points and 0 elsewhere. We can then represent the function, $\overline{\Phi} \in V_h$ as:

$$\overline{\Phi} = \sum_{i=1}^{N} \alpha_i \Psi(x_i) \tag{6}$$

such that $\overline{\Phi} \in V_h$ can be written in a unique way as a linear combination of the basis functions $\Psi_i \in V_h$. The finite element approximation of the original boundary value problem (1) can be stated as:

$$\text{Find } \Phi_h \in V_h \text{ such that } (\sigma \nabla \Phi_h, \nabla \overline{\Phi}) = -(I_v, \overline{\Phi}). \tag{7}$$

Furthermore, since $\Phi_h \in V_h$ satisfies (7), then we have $(\sigma \nabla \Phi_h, \nabla \Psi) = -(I_v, \Psi_i)$. Finally, since Φ_h itself can be expressed as the linear combination:

$$\Phi_h = \sum_{i=1}^{N} \xi_i \Psi_i(x) \quad \xi_i = \Phi_h(x_i), \tag{8}$$

we can then write (7) as:

$$\sum_{i=1}^{N} \xi_i (\sigma_{ij} \nabla \Psi_i, \nabla \Psi_j) = -(I_v, \Psi_j) \quad j = 1, \ldots, N. \tag{9}$$

The finite element approximation of (1) can equivalently be expressed as a system of N equations with N unknowns, $\xi_1, \ldots, \xi_N$ (the electrostatic potentials). In matrix form, the above system is expressed as $A\xi = b$, where $A = (a_{ij})$ is the global stiffness matrix and has elements $(a_{ij} = (\sigma_{ij} \nabla \Psi_i, \nabla \Psi_j))$, while $b_i = -(I_v, \Psi_i)$ is the vector of source contributions.

Adaptive Methods

Discrete approaches to bioelectric inverse and imaging problems have centered around classical numerical techniques for solving partial differential equations: finite difference, finite element, and boundary element methods. To date, instead of developing and utilizing specific, quantitative methods, most bioengineers have assigned spatial discretization levels by relying largely on previous experience and their common sense, utilizing what has apparently worked before and perhaps reducing the discretization level in regions *a priorily* known to contain high gradients. This situation has arisen, at least in part, because of the computational load represented by the large, complex, inhomogeneous, even anisotropic geometries that characterize many problems in bioelectric field imaging.

We have found, however, that by using *a posteriori* estimates from the finite element approximation of the governing equations, along with a minimax theorem to determine the stopping criterion, we can locally refine the discretization and reduce the errors in the direct solution. It has always been assumed — and our findings support this notion — that improving the accuracy of the direct solution also improves the subsequent inverse solution. The novel aspect of our approach is that it uses local approximations of the error in the numerical solutions to drive an automatic adaptive mesh refinement [3, 4].

Mathematically, we can obtain an error estimator by starting from the *weak formulation* of the finite element approximation, (7). We can prove that $\Phi_h \in V_h$ (where Φ_h is the finite element solution and related to ξ by (8)) is the best approximation of the exact solution Φ in the sense that

$$\|\nabla \Phi - \nabla \Phi_h\| \leq \|\nabla \Phi - \nabla \tilde{\Phi}\| \quad \forall\, \tilde{\Phi} \in V_h \tag{10}$$

where

$$\|\nabla \tilde{\Phi}\| = (\int_{\Omega} \nabla \tilde{\Phi} \cdot \nabla \tilde{\Phi})^{\frac{1}{2}}. \tag{11}$$

In particular, we can choose $\tilde{\Phi}$ to be the interpolant of Φ

$$\pi_h \Phi(N_i) = \Phi(N_i) \qquad i = 1, \ldots, M \quad \pi_h \Phi \in V_h. \tag{12}$$

This says that the error in the finite element approximation is bounded from above by the interpolation error. With certain constraints on our elements, we can prove the following, well know relationships:

$$\|\nabla \Phi - \nabla \pi_h \Phi\| \leq Ch \tag{13}$$

and

$$\|\Phi - \pi_h\Phi\| \leq Ch^2 \tag{14}$$

where C is a positive constant that depends on the size of the second partial derivative of Φ and the smallest angle formed by the sides of the elements in V_h. These estimates show that the error in both Φ and the gradient of Φ tend to zero as the discretization parameter, h, tends to zero. We can use these relationships to provide an adaptive algorithm for decreasing discretization error.

To make this a little more precise, we define the semi-norm:

$$|\tilde{\Phi}|_{H^r(\Omega)} = (\sum_{|\alpha|=r} \int_\Omega |D^\alpha \tilde{\Phi}|^2 \, dx)^{\frac{1}{2}} \tag{15}$$

where

$$D^\alpha \tilde{\Phi} = \frac{\partial^{|\alpha|}\tilde{\Phi}}{\partial x_1^{\alpha_1} \partial x_2^{\alpha_2}} \qquad |\alpha| = \alpha_1 + \alpha_2 \tag{16}$$

are α-order partial derivatives and

$$H^K(\Omega) = \{\tilde{\Phi} \in L_2(\Omega) : \; D^\alpha \tilde{\Phi} \in L_2(\Omega), \; |\alpha| \leq K\} \tag{17}$$

defines the Sobolev spaces. Given these definitions, we can then obtain the error estimates analogous to those in (13) and (14) for the finite element approximation [5, 6]:

$$|\Phi - \Phi_h|_{H^1(\Omega)} \leq |\Phi - \pi_h\Phi|_{H^1(\Omega)} \leq C[\sum_{K \in T_n} (h_k |\Phi|_{H^2(K)})^2]^{\frac{1}{2}} \tag{18}$$

or, in the $L_2(\Omega)$ norm,

$$\|\Phi - \Phi_h\|_{L_2(\Omega)} \leq \|\Phi - \pi_h\Phi\|_{L_2(\Omega)} \leq Ch^2 |\Phi|_{H^2(\Omega)}. \tag{19}$$

For the potential gradients we have [7]:

$$\|\nabla\Phi - \nabla\Phi_h\|_{L_{\infty(\Omega)}} \leq C\|\nabla\Phi - \nabla\pi_h\tilde{\Phi}\|_{L_{\infty(\Omega)}} \leq C \max[h_K \max_{\alpha=2} \|D^\alpha\Phi\|_{L_{\infty(\Omega)}}]. \tag{20}$$

Given these previous error estimates for the finite element approximation, we can now use the estimates to decide where in our original finite element mesh the approximation is not accurate and create a recursive, adaptive algorithm to re-discretize in the appropriate areas. Suppose we want the accuracy of our finite element approximation to be within some given tolerance, δ, of the true solution, i.e.

$$|\Phi - \Phi_h|_{H^1(\Omega)} \leq \delta. \tag{21}$$

Then, we redefine our mesh until,

$$\sum_{K \in T_h} (h_k |\Phi_h|_{H^2(K)})^2 \leq \frac{\delta^2}{C^2}. \tag{22}$$

Here the sum is over all the K elements in the tessellated geometry, T_h, and we test to see if the error is less than the *normalized* tolerance. If the value of the error estimate exceeds the tolerance, the element is 'flagged' for further refinement. The refinement can occur either by further subdividing the egregious element (so-called h-adaption) or by increasing the basis function of the element (p-adaption), or both (hp-adaption). One should note that the $H^2(\Omega)$ norm in (22) requires the second partial derivative of the finite element approximation. As stated in (8), we have

assumed a linear basis function for our fundamental element. Thus, there is no continuity of the second derivative and we must approximate it using a centered difference (or other) formula based on first derivative information.

Of significant practical importance is the choice of a reasonable tolerance, δ. Since the general location and bounds of the potential field are dictated by known physiological considerations, we can generate an initial mesh based upon simple field strength-distance arguments. To estimate an upper bound of the potential (or electric) field we can find the field strength on a cylindrical surface which encloses the actual geometry. The result is an estimate of the potential field and potential gradients which are used to produce the initial graded mesh. The goal of this calculation is to assure that the errors far from the sources are minimal. We can then refine our finite element mesh by choosing the tolerance, δ, to be some fraction of the estimated error corresponding to the elements furthest from the sources. Thus we have used a minimax principle, minimizing the maximum error based upon initial (conservative) estimates of the potential field and potential gradients [3].

Regularization

Traditional schemes for solving the inverse problem, (3), have involved reformulating the linear equation, $A\xi = b$, into $\xi_T = K\xi_E$, where ξ_T and ξ_E are the voltages on the body surface (torso) and heart's surface (epicardium) respectively, and K is the $T \times E$ transfer matrix of coefficients relating the measured torso voltages to the voltages measured on the heart. From this statement of the forward problem, the inverse problem can then be expressed as $\xi_E = K^{-1}\xi_T$

Unfortunately, K is ill-conditioned, and regularization techniques are necessary to restore continuity of the solution back onto the data. To date, all regularization schemes have focused on treating K globally and using Tikhonov, singular value decomposition (SVD), or Twomey algorithms with a single regularization parameter. Briefly, one wishes to find an approximate vector, $\xi_{E\varepsilon}$, such that $\xi_{E\varepsilon} \to \xi_E$ as $\varepsilon \to 0$, where ε is the error between the approximate and true values. It is possible to reformulate the K matrix into an expression involving sub-matrices of K. We have found that it is then possible, and advantageous, to apply regularization not globally, but at the *local* level of the submatrices.

Researchers have long noticed that the discontinuities in the inverse solution appear irregularly distributed throughout the data. Tikhonov and other regularization schemes are, in effect, filters, which restore continuity by attenuating the high (spatial) frequency components of the solution. Since regularization is usually applied globally, the results can leave some regions overly damped or smoothed while others remain poorly constrained. Our idea is then to apply regularization only to sub-matrices that require it and to apply different amounts of regularization to different sub-matrices.

We begin by expressing $A\xi = b$ for the Cauchy problem in (3) as

$$\begin{pmatrix} A_{TT} & A_{TV} & A_{TE} \\ A_{VT} & A_{VV} & A_{VE} \\ A_{ET} & A_{EV} & A_{EE} \end{pmatrix} \begin{pmatrix} \xi_T \\ \xi_V \\ \xi_E \end{pmatrix} = \begin{pmatrix} 0 \\ 0 \\ 0 \end{pmatrix}. \tag{23}$$

We can then rearrange the matrix to solve directly for the epicardial voltages in terms of the measured body surface voltages,

$$\xi_E = (A_{TV}A_{VV}^{-1}A_{VE} - A_{TE})^{-1}(A_{TT} - A_{TV}A_{VV}^{-1}A_{VT})\xi_T, \tag{24}$$

where the subscripts T, V, and E stand for the nodes in the regions of the torso, the internal volume, and epicardium, respectively. Since torso and epicardial nodes are always separated by

more than one element, the A_{TE} submatrix is zero, and we can then rewrite (24) as

$$\xi_E = (A_{VE}^{-1} A_{VV} A_{TV}^{-1})(A_{TT} - A_{TV} A_{VV}^{-1} A_{VT})\xi_T. \tag{25}$$

Note that we now have inverses of three sub-matrices, A_{VE}, A_{TV}, and A_{VV}, as well as several other matrix operations to perform. If one estimates the condition number, κ, of the three sub-matrices using the ratio of the maximum to minimum singular values from a singular value decomposition (SVD), one finds that the condition number varies significantly (from $\kappa \approx 200$ for A_{VV} to $\kappa \approx 1 \times 10^{16}$ for A_{VE} in the two-dimensional model described below). Thus, one can regularize each of the sub-matrices differently, even leaving some of the other sub-matrices untouched. The overall effect of this *local regularization* is more control over the regularization process.

Since the goal of the inverse problem in electrocardiography is to accurately and noninvasively (i.e., non-surgically) estimate the voltages on the epicardial surface, we need a method to choose an optimal regularization parameter *a priorily*. Traditional schemes have been based on discrepancy principles [8], quasi-optimality criterion [8, 9], and generalized cross-validation [10]. Recently, Hansen [11] has extended the observations of Lawson and Hanson [12] and proposed a new method for choosing the regularization parameter based on an algorithm that locates the "corner" of a plot of the norm (or semi-norm) of the regularized solution, $\|Lx_\alpha\|$, versus the norm of the corresponding residual vector, $\|Ax_\alpha - b\|$. In this way, one can evaluate the compromise between the minimization of the two norms. We have utilized the *L-curve* algorithm along with our local Tikhonov regularization scheme to improve the accuracy of solutions to the inverse problem.

For the global Tikhonov regularization scheme, we can find an estimate for $\xi_{E\varepsilon}$ by minimizing a generalized form of the Tikhonov functional:

$$M^\alpha[\xi_E, \tilde{\xi}_T, \tilde{K}] = \|K\xi_E - \tilde{\xi}\|_{\phi_T}^2 + \alpha\|C(\xi_E - \xi_E^{'})\|_{\phi_E}^2 \quad \alpha > 0 \tag{26}$$

in terms of the epicardial potentials,

$$\xi_{E\varepsilon}^\alpha = [\tilde{K}^T\tilde{K} + \alpha C^T C]^{-1}[\tilde{K}^T\tilde{\xi}_T + \alpha C^T C\xi_E^{'}] \tag{27}$$

where $\tilde{K}$ is the approximation of the true transformation matrix, K, $\tilde{\xi}_T$ are the measured torso potential values, $\xi_E^{'}$ are *a priori* constraints placed on the epicardial potentials based on physiological considerations, C is a constraint matrix (either the identity matrix, a gradient operator, or a Laplacian operator), and α is the regularization parameter. For our *local* regularization scheme, we replace the global matrix, K, by the two sub-matrices A_{VE} and A_{TV} from (25). We note that A_{VV} in (25) has a stable inverse and, thus, does not need regularizing.

Results and Discussion

To study the direct and inverse problems in electrocardiography, we developed a series of two- and three-dimensional boundary element and finite element models based upon magnetic resonance images from a human subject. Each of 116 MRI scans were segmented into contours defining torso, fat, muscle, lung, and heart regions. Additional node points were added to digitize each layer and pairs of layers tessellated into tetrahedra using a Delaunay triangulation algorithm [13, 14]. The resulting model of the human thorax contained approximately 675,000 volume elements, each with a corresponding conductivity tensor. For the initial studies on the effects of adaptive control of errors and local regularization, we utilized a two-dimensional finite element model extracted from our three-dimensional model of the human thorax. The two-dimensional model was constructed

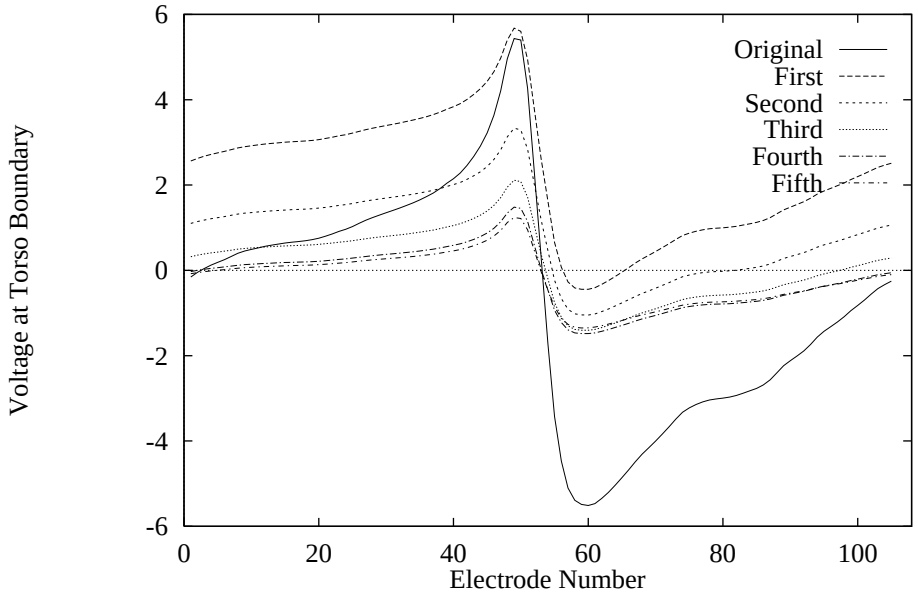

Figure 1: Effects of Automatic Mesh Refinement

from a single transaxial magnetic resonance image located approximately 4 cm. above the apex of the heart.

As a test of the adaptive algorithm, a simulated source distribution was placed on the surface of the heart model. Using the procedure described previously, direct solutions were computed for different levels of mesh refinement and compared at the outer torso boundary. Figure 1 shows the voltage at the outer boundary versus distance around the two-dimensional contour. The original mesh contained approximately 1500 elements while the final mesh, after five iterations of the adaptive algorithm, contained approximately 7000 elements. The maximum estimated error in the calculated potential was over 30% greater in the original mesh compared to the final mesh and the maximum estimated error in the potential gradient was over 13% larger in the original mesh compared to the refined mesh. Increased accuracy does not come without a price and the h-adaption increases the number of degrees of freedom, and thus, the computational costs. One must balance accuracy against CPU time. However, since the relative error falls off rapidly with increasing degrees of freedom and then levels out after only a few iterations of the adaptive algorithm, it is not difficult to choose a reasonable balance.

As a test of the local regularization we applied epicardial potentials recorded during open chest surgery from a patient diagnosed with WPW syndrome as the Dirichlet boundary conditions of the two-dimensional model described above. The tissue conductivities were assigned as follows: fat = .045 S/m, fatpad = .045 S/m, lungs = .096 S/m, skeletal muscle (along the fiber) = .3 S/m, skeletal muscle (across the fiber) = .1 S/m, and an average thorax value = .24 S/m. Forward solutions calculated using the adapted mesh served as torso boundary conditions, $\Phi = \Phi_0$ on $\Sigma \subseteq \Gamma_T$ for the inverse solution.

For the sub-matrices A_{VE} and A_{TV} the *L-curve* algorithm determined the optimal *a priori* regularization parameter. The local Tikhonov regularization technique was then applied to the two sub-matrices and the inverse solution matrix computed. Because the size of the two-dimensional finite element model was relatively small, the calculations stayed in dynamic memory on an IBM

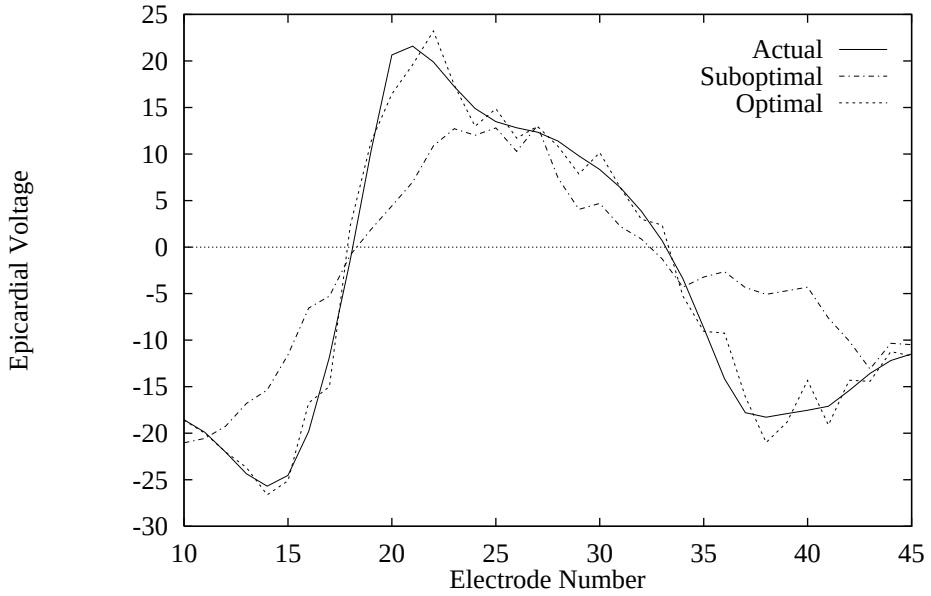

Figure 2: Local Regularization Technique

RISC-6000 model 580 (we note that for the three-dimensional models a distributed iterative algorithm will be utilized to achieve realistic computation times. The resulting inverse solutions were then compared to those calculated using standard global Tikhonov techniques and the original measured epicardial potentials.

The application of the local regularization technique recovered the voltages to within 12.6% RMS error. Previous studies have reported the recovery of epicardial potentials with errors in the range of 20-40%, [15, 16, 17, 18]. Figure 2 shows the inverse solution calculated using the local regularization technique compared with the recorded heart voltages as a function of position on the epicardium. The global solution tended to be smoother, not able to follow the extrema as well as the local solution could. The local solution also showed areas of local error which suggest that a different partitioning of the sub-matrices may provide even better accuracy.

In interpreting the results of the local regularization method, we must plead guilty to several *inverse crimes*. Namely, we have used the same finite element mesh to calculate solutions for both the forward and inverse problem, and we have not, at this point, added noise to the input torso boundary values. Currently, we are investigating the effects of added noise on a variety of experimental data as well as developing more general and computationally efficient ways to decompose the transfer matrix. Of particular interest is a method which employs a parallel block LU decomposition algorithm. Other investigations include methods with which to automatically determine which partitioning of the matrix yields the most accurate solutions and how the computations may be best distributed over multiple processors.

Acknowledgments

This research was supported in part by awards from the Whitaker Foundation, NIH Grant HL47505, the Nora Eccles Treadwell Foundation, and the Richard A. and Nora Eccles Harrison Fund for

Cardiovascular Research. The authors would like to thank K. Coles and C. Gitlin for their comments and suggestions. Portions of the paper were excerpted from C.R. Johnson and R.S. Macleod, Inverse solutions for electric and potential field imaging, in R.L. Barbour and M.J. Carvlin, eds., *Physiological Imaging, Spectroscopy, and Early Detection Diagnostic Methods*, vol. 1887, SPIE, pp. 130-139, 1993.

References

[1] Y. Yamashita. Theoretical studies on the inverse problem in electrocardiography and the uniqueness of the solution. *IEEE Trans Biomed Eng*, BME-29:719–725, 1982.

[2] R.S. MacLeod, C.R. Johnson, and B.M. Gardner, M.J. Horáček. Localization of ischemia during coronary angioplasty using body surface potential mapping and an electrocardiographic inverse solution. In *Computers in Cardiology*, pages 251–254. IEEE Press, 1992.

[3] C.R. Johnson and R.S. MacLeod. Nonuniform spatial mesh adaption using a posteriori error estimates: applications to forward and inverse problems. *Applied Numerical Mathematics*, 14:311–326, 1994.

[4] J.A. Schmidt, C.R. Johnson, J.C. Eason, and R.S. MacLeod. Applications of automatic mesh generation and adaptive methods in computational medicine. In J.E. Flaherty and I. Babuska, editors, *Modeling, Mesh Generation, and Adaptive Methods for Partial Differential Equations*. Springer-Verlag, 1994 (to appear).

[5] P.G. Ciarlet and J.L Lions. *Handbook of Numerical Analysis: Finite Element Methods*, volume 1. North-Holland, Amsterdam, 1991.

[6] C. Johnson. *Numercial solution of Partial Differential Equations by the Finite Element Method*. Cambridge University Press, Cambridge, 1990.

[7] R. Rannacher and R. Scott. Some optimal error estimates for piecewise linear finite element approximations. *Math. Comp.*, 38:437–445, 1982.

[8] V.A. Morozov. *Methods for Solving Incorrectly Posed Problems*. Springer-Verlag, New York, 1984.

[9] R. Kress. *Linear Integral Equations*. Springer-Verlag, New York, 1989.

[10] G.H. Golub, M.T. Heath, and G. Wahba. Generalized cross-validation as a method for choosing a good ridge parameter. *Technometrics*, 21:215–223, 1979.

[11] P.C. Hansen. Analysis of discrete ill-posed problems by means of the L-curve. *SIAM Review*, 34(4):561–580, 1992.

[12] C.L. Lawson and R.J. Hanson. *Solving Least Squares Problems*. Prentice-Hall, Englewood Cliffs, NJ, 1974.

[13] C.R. Johnson, R.S. MacLeod, and P.R. Ershler. A computer model for the study of electrical current flow in the human thorax. *Computers in Biology and Medicine*, 22(3):305–323, 1992.

[14] C.R. Johnson, R.S. MacLeod, and M.A. Matheson. Computer simultions reveal complexity of electrical activity in the human thorax. *Comp. in Physics*, 6(3):230–237, May/June 1992.

[15] F.P. Colli Franzone, G. Gassaniga, L. Guerri, B. Taccardi, and C. Viganotti. Accuracy evaluation in direct and inverse electrocardiology. In P.W. Macfarlane, editor, *Progress in Electrocardiography*, pages 83–87. Pitman Medical, 1979.

[16] P. Colli Franzone, L. Guerri, S. Tentonia, C. Viganotti, S. Spaggiari, and B. Taccardi. A numerical procedure for solving the inverse problem of electrocardiography. Analysis of the time-space accuracy from *in vitro* experimental data. *Math Biosci*, 77:353, 1985.

[17] B.J. Messinger-Rapport and Y. Rudy. Regularization of the inverse problem in electrocardiography: A model study. *Math Biosci*, 89:79–118, 1988.

[18] P.C. Stanley, T.C. Pilkington, and M.N. Morrow. The effects of thoracic inhomogeneities on the relationship between epicardial and torso potentials. *IEEE Trans Biomed Eng*, BME-33:273–284, 1986.